ChemComm

CrossMark
← click for updates

Sc₃CH@C₈₀: selective ^{13}C enrichment of the central carbon atom†

Katrin Junghans, Marco Rosenkranz and Alexey A. Popov*

Sc₃CH@C₈₀ is synthesized and characterized by ^{1}H, ^{13}C, and ^{45}Sc NMR. A large negative chemical shift of the proton, -11.73 ppm in the I_h and -8.79 ppm in the D_{5h} C₈₀ cage isomers, is found. ^{13}C satellites in the ^{1}H NMR spectrum enabled indirect determination of the ^{13}C chemical shift for the central carbon at 173 ± 1 ppm. Intensity of the satellites allowed determination of the ^{13}C content for the central carbon atom. This unique possibility is applied to analyze the cluster/cage ^{13}C distribution in mechanistic studies employing either ^{13}CH₄ or ^{13}C powder to enrich Sc₃CH@C₈₀ with ^{13}C.

The pressure of helium gas is one of the most important parameters affecting the yield of fullerenes in arc-discharge synthesis. Optimization of the atmosphere in the arc-discharge generator (both the pressure and composition) is even more crucial for the synthesis of endohedral metallofullerenes (EMFs) and clusterfullerenes, whose yields are usually much lower than those of empty fullerenes.[1] New types of fullerenes or their derivatives can be obtained by introducing different reagents into the arc. Stevenson *et al.* were the first to show that in the presence of molecular nitrogen, the nitride clusterfullerene Sc₃N@C₈₀ can be synthesized in appreciable yield.[2] Then, Dunsch *et al.* demonstrated advantages of the reactive atmosphere method in the synthesis of EMFs: the use of NH₃ as a source of nitrogen not only afforded the synthesis of nitride clusterfullerenes, but also suppressed the yield of empty fullerenes.[3] The method was adopted for the synthesis of other types of EMF clusterfullerenes, such as sulfides,[4] oxides,[5] or certain types of carbides.[6–9] It was also applied to stabilize unconventional empty fullerene cages *via* their *in situ* derivatization by hydrogen[10] or chlorine atoms.[11] Interestingly, whereas the use of SO₂ or CO gases for the synthesis of clusterfullerenes leads to a large amount of empty fullerenes, the hydrogen-containing reagents (NH₃, CH₄, solid organic compounds[12]) suppress the yield of empty fullerenes.

Leibniz Institute for Solid State and Materials Research, 01069 Dresden, Germany.
E-mail: a.popov@ifw-dresden.de

† Electronic supplementary information (ESI) available: Additional experimental details, HPLC separation, FTIR and NMR spectra. See DOI: 10.1039/c5cc10025a

Recently we have shown that methane can be advantageous for the synthesis of carbide clusterfullerenes, such as M₂TiC@C₈₀ or M₂TiC₂@C₈₀ (M is Y or a lanthanide).[8] It is not clear if methane is barely a source of hydrogen suppressing the empty fullerene formation, or it plays a more specific role by, *e.g.*, supplying the carbon for the endohedral cluster. Answering this question may shed more light on the fullerene formation, but the analysis of the carbon source in the EMF molecule is not straightforward. The use of isotopic substitution would be an obvious way to address this problem, but mass-spectrometry is not able to distinguish the cage and cluster atoms, whereas sensitivity of ^{13}C NMR is not sufficient to allow distribution studies (detection of the central carbon atoms in carbide clusterfullerenes by ^{13}C NMR required ^{13}C enrichment[9,13–15]). Here we circumvent this problem by studying the Sc₃CH@C₈₀, which affords ^{13}C analysis of the central carbon *via* the ^{1}H NMR signal of the endohedral hydrogen and show that methane plays an active role in the formation of the endohedral cluster.

Sc₃CH@C₈₀ was synthesized in two series of experiments, using either pure Sc or a 1 : 1 mixture of Sc and Ti, as a source of metal. Metals were mixed with graphite powder and packed into the hole-drilled graphite rods, which were then used in the arc-discharge synthesis in the He atmosphere with an addition of several mbar of CH₄ (250 mbar total pressure). The main EMF products of the arc discharge synthesis in these conditions are Sc₄C₂@C₈₀ in pure Sc system, and Sc₂TiC@C₈₀ in the mixed-metal Sc/Ti system. Both systems afforded appreciable amounts of Sc₃CH@C₈₀, which was further isolated using HPLC (see ESI† for further details of separation).

Detailed characterization of Sc₃CH@C₈₀ in the first report on its synthesis was not possible due to the tiny amounts of the isolated compound.[6] In this work, we accomplished characterization of the compound by ^{45}Sc, ^{13}C, and ^{1}H NMR spectroscopy as shown in Fig. 1. The icosahedral cage symmetry of Sc₃CH@C₈₀ is proved by ^{13}C NMR spectroscopy (Fig. 1a). Two cage resonances with the 3 : 1 intensity ratio are observed at 144.06 and 136.78 ppm, which is close to the chemical shifts reported for other cluster-fullerenes with the C₈₀-I_h cage[2,16–19] (144.57/137.24 ppm in
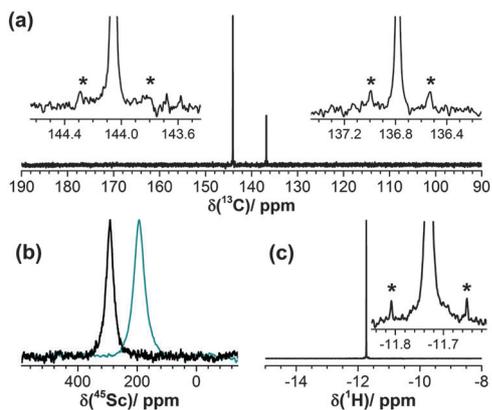
Fig. 1 NMR spectra of $Sc_3CH@C_{80}$ dissolved in CS_2: (a) 125 MHz ^{13}C NMR; (b) 121.5 MHz ^{45}Sc NMR (black line – $Sc_3CH@C_{80}$, cyan line – $Sc_3N@C_{80}$); (c) 500 MHz ^1H NMR. The insets in (a) and (c) show ^{13}C satellites marked with asterisks.

$Sc_3N@C_{80}$,[2] 144.7/137.8 in $Sc_4C_2@C_{80}$,[17] 144.9/137.7 ppm in $Sc_3CN@C_{80}$,[18] or 144.82/137.29 ppm in $Sc_4O_2@C_{80}$[19]). In the ^{13}C-enriched sample, satellite peaks due to coupling of neighboring cage atoms can be seen (Fig. 1a) with the $^1J_{CC}$ coupling constant of 58 Hz, typical for C-sp^2 carbon atoms in conjugated π-systems.[20] Presumably, the large line-width of the endohedral carbon signal[14] did not allow us to detect it in the direct ^{13}C NMR measurements, and the chemical shift of the endohedral carbon was determined from selective decoupling measurements of ^1H NMR (see below).

In ^{45}Sc NMR spectrum, $Sc_3CH@C_{80}$ exhibits a single resonance at 292 ppm (Fig. 1b). This value is 100 ppm low-field with respect to the ^{45}Sc chemical shift in $Sc_3N@C_{80}$ at 191 ppm (Fig. 1b). The proton NMR signal of $Sc_3CH@C_{80}$ was detected at −11.73 ppm (Fig. 1c). Such a high-field value is typical for endohedral protons[21–24] (see Table 1). We also detected formation of the second isomer of $Sc_3CH@C_{80}$, presumably with the D_{5h} carbon cage (Fig. S6, ESI†), whose ^1H NMR signal is detected at −8.79 ppm.

The ^1H NMR spectrum of $Sc_3CH@C_{80}$ also exhibits a low intensity doublet due to the proton-bonded ^{13}C (Fig. 1c). The $^1J_{C–H}$ coupling constant is small, 78.5 Hz, which is typical for protons bonded to carbon atoms with highly electropositive substituents. Thus, the measured $^1J_{C–H}$ constant is in line with the large negative charge on the central carbon atom predicted for $Sc_3CH@C_{80}$.[27] The possibility to detect ^{13}C satellites in the proton NMR spectrum enables determination of the ^{13}C

chemical shift of the central carbon atom via ^1H NMR measurements with selective ^{13}C decoupling at different ^{13}C irradiation frequencies. The satellites are well visible at 165 or 180 ppm, but disappear completely at 172–175 ppm (Fig. S4, ESI†). Thus, the ^{13}C chemical shift of the central atom in $Sc_3CH@C_{80}$ is determined as 173 ± 1 ppm, which is noticeably downfield than ^{13}C chemical shifts of endohedral carbons in carbide clusterfullerenes (see Table 1).

Sc_3CH and Sc_3N clusters have the same formal charge (6+) and identical electron count (the $(C–H)^{3-}$ unit is analogous to the nitride ion N^{3-}), and therefore a close similarity of the electronic properties of $Sc_3CH@C_{80}$ and $Sc_3N@C_{80}$ can be expected.[6,27] Indeed, both compounds exhibit very similar Vis-NIR absorption spectra (Fig. 2a), with a slight blue shift of the lowest energy band in $Sc_3CH@C_{80}$ (717 nm versus 734 nm in $Sc_3N@C_{80}$). The difference is more distinct in the fluorescence spectra: whereas $Sc_3CH@C_{80}$ exhibits a NIR emission band at 835 nm, the maximum of the fluorescence band of $Sc_3N@C_{80}$ is observed at 910 nm. Crossing points of the absorption and emission bands give the optical gaps of $Sc_3CH@C_{80}$ and $Sc_3N@C_{80}$ as ca. 1.62 and 1.53 eV, respectively. The electrochemical gap of $Sc_3CH@C_{80}$ is also 0.09 V larger than that of $Sc_3N@C_{80}$ (Fig. 2b and Table 2). Both compounds exhibit similar redox behaviour with chemically irreversible first reduction near −1.2 V. DFT calculations show that $Sc_3CH@C_{80}$
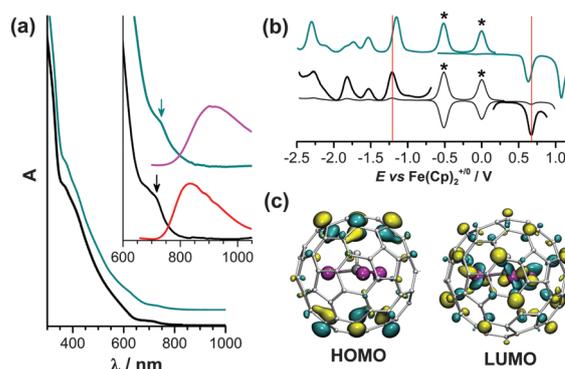

Fig. 2 (a) UV-Vis spectra of $Sc_3CH@C_{80}$ (black) and $Sc_3N@C_{80}$ (cyan) in toluene, the inset shows absorption spectra in the range of the lowest energy transitions and luminescence spectra ($Sc_3CH@C_{80}$ – red, $Sc_3N@C_{80}$ – magenta; laser excitation at $λ_{ex}$ = 405 nm); (b) square wave voltammetry of $Sc_3CH@C_{80}$ (black) and $Sc_3N@C_{80}$ (cyan) in o-dichlorobenzene/TBABF$_4$, asterisks mark $Fe(Cp)_2$ and $Fe(Cp^*)_2$ used as internal standards; to guide an eye, the first reduction and oxidation potentials of $Sc_3CH@C_{80}$ are denoted with vertical red lines; (c) HOMO and LUMO of $Sc_3CH@C_{80}$ computed at the PBE/def2-TZVP level.[28]

Table 1 ^1H and ^{13}C chemical shifts (ppm) for endohedral clusters in $Sc_3CH@C_{80}$ and selected endohedral fullerenes

EMF	$δ(^1H)$	Ref.	EMF	$δ(^{13}C)$	Ref.
$Sc_3CH@C_{80}$-I^a	−11.73		$Sc_3CH@C_{80}$-I^a	173 ± 1	
$Sc_3CH@C_{80}$-II^a	−8.79		$M_2C_2@C_{2n}$^{b}	220–260	13–15 and 25
$H_2@C_{60}$	−1.44	21	$YCN@C_{82}$	292.4	26
$H_2O@C_{60}$	−4.81	22	$Sc_3C_2@C_{80}$$^-$	328.3	14
$H_2@C_{70}$	−23.97	23	$Lu_2TiC@C_{80}$	340.98	9

^{a} $Sc_3CH@C_{80}$-I and $Sc_3CH@C_{80}$-II denote the major (I_h) and the minor (presumably D_{5h}) isomers. ^{b} M = Sc, Y; $2n$ = 80, 82, 84, 92.

Table 2 Redox potentials (V) of $Sc_3CH@C_{80}$ and $Sc_3N@C_{80}$^{a}

EMF	O-II	O-I	R-I	R-II	R-III	Gap$_{EC}$
$Sc_3CH@C_{80}$		0.67	−1.21	−1.53/−1.82	−2.28	1.88
$Sc_3N@C_{80}$	1.09	0.63	−1.15	−1.54/−1.73		1.79

^{a} All potentials are determined by square-wave voltammetry in o-dichlorobenzene/TBABF$_4$ and are referred versus $Fe(Cp)_2^{+/0}$ redox couple; "O" and "R" denote oxidation and reduction, respectively.

and Sc$_3$N@C$_{80}$ have almost identical spatial distribution of the HOMO and LUMO. The HOMO is essentially a carbon cage orbital, whereas the LUMO has large contribution of Sc atoms (Fig. 2c).

Sc$_3$CH@C$_{80}$ offers a unique possibility to study the role of methane in the carbide clusterfullerene formation using ^{13}C-enrichment. The isotopic distribution of the central carbon atom can be determined by ^{1}H NMR from the intensity of the ^{13}C satellites, whereas the net isotopic distribution in the whole molecule (dominated by that of the carbon cage) can be deduced from the mass-spectra. We synthesized ^{13}C-enriched Sc$_3$CH@C$_{80}$ by applying either (i) ^{13}CH$_4$ or (ii) ^{13}C powder. To distinguish the two series, they will be denoted as "^{13}CH$_4$/C" and "CH$_4$/^{13}C", respectively. The amount of ^{13}C powder in the CH$_4$/^{13}C series was adjusted to keep the same amount of ^{13}C in the generator as in the ^{13}CH$_4$/C series. Fig. 3 compares ^{1}H NMR and mass-spectra of the Sc$_3$CH@C$_{80}$ sample synthesized with the natural-abundant CH$_4$/C to the two types of ^{13}C-enriched samples, whereas estimated ^{13}C content is summarized in Table 3. In the CH$_4$/^{13}C syntheses, the isotopic composition for the central atom and the whole molecule are both equal 5–6% within the uncertainty limits of the NMR measurements (ca. 1%). Thus, the carbon originating from the powder is equally distributed between the cage and the central atom; similar conclusion was achieved by Dorn et al. in their mass-spectrometric study of the empty fullerenes and Y–carbide clusterfullerenes.[15]

Substantially different results are obtained in the ^{13}CH$_4$/C syntheses: the ^{13}C enrichment of the carbon cage is only 1.6 ± 0.1%, whereas the ^{13}C content for the central atoms is much higher, 7.6 ± 1.5%. Thus, despite the rather large error bars in

the NMR measurement (caused by the limited sample amount), selective ^{13}C enrichment of the central carbon atom by ^{13}CH$_4$ is beyond any doubt. The ^{13}CH$_4$/C syntheses thus provide rich information on the Sc$_3$CH@C$_{80}$ formation process.

The volume inside the generator can be schematically divided into three zones:

(1) The "hot" zone near the center of the arc, where the temperature is up to several thousand K,[29] and majority of chemical bonds (including C–H) are broken. Only the most stable species (such as C$_2$ dimers) can survive.

(2) The periphery of the hot zone, where the carbon vapor cools down by the adiabatic expansion and interaction with helium atoms, resulting in a self-assembly of fullerenes and other carbonaceous structures. This intermediate zone is hot enough to provide sufficient energy for the rearrangement of the building carbon networks, but the temperature is not high enough for their atomization.

(3) The "cold" zone, where the fullerenes can only anneal (e.g., structural defects can be healed), but substantial structural rearrangements are already not possible.

We propose that all CH$_4$ molecules entering the hot zone are completely atomized, and therefore the carbon atoms from methane can serve as a source of carbon for the fullerene cage. Since the hot zone occupies only a small volume, whereas methane is distributed over the whole generator chamber, only a small fraction of methane present in the system passes through the hot zone. Thus, it is not surprising that the content of methane-originating carbon atoms in the fullerene cage is not exceeding 0.5%, whereas the main sources of carbon for both the fullerene cage and the endohedral cluster are the graphite rods and graphite powder packed into the rods.

When the C/H vapor leaves the hot zone, the CH bonds can be formed again. Note that from the 0.5% contribution of the methane as a source of carbon for the cage, the C : H ratio in the hot zone is tentatively estimated as 50 : 1. This ratio is sufficient for a dramatic suppression of the empty fullerene formation. The ^{13}C/^{12}C distribution in the newly formed CH bonds can be considered roughly equal the ^{13}C content in the carbon cage (1.6% in the ^{13}CH$_4$/C syntheses). The fact that the ^{13}C content for the central carbon atom in Sc$_3$CH@C$_{80}$ obtained in the ^{13}CH$_4$ syntheses is several times higher than for the fullerene cage means that methane is also chemically active in the "intermediate" zone. Although CH$_4$ molecules are not completely atomized here, they can exchange protons with other carbon structures or react with Sc atoms to substitute protons. However, some ^{13}CH fragments remain intact (else the isotopic distribution for the cage and the cluster would be equalized) and take part in the endohedral fullerene formation. The fraction of such "native" ^{13}CH units in Sc$_3$CH@C$_{80}$ is the difference between the ^{13}C content in the cluster and in the cage, and can be roughly estimated as 6%.

In this work we reported on the synthesis and spectroscopic characterization of Sc$_3$CH@C$_{80}$. Its ^{13}C, ^{45}Sc, and ^{1}H NMR spectra are reported for the first time and fully establish the molecular structure of this clusterfullerene. Electronic properties of Sc$_3$CH@C$_{80}$ are similar to those of its close analog,

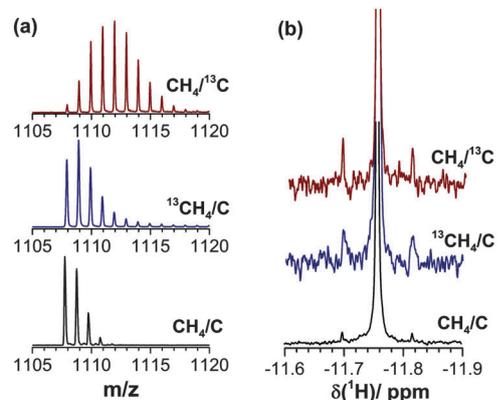Fig. 3 (a) Mass-spectra of Sc$_3$CH@C$_{80}$ samples with different ^{13}C content obtained in CH$_4$/^{13}C, ^{13}CH$_4$/C, and CH$_4$/C syntheses; (b) ^{1}H NMR spectra for the same samples, normalized to the intensity of the main singlet.

Table 3 ^{13}C content for the central atom and the whole molecule

^{13}C enrichment	^{1}H NMR (%)	Mass-spectrometry (%)
C/CH$_4$[a]	1.1 ± 0.4	1.1 ± 0.1
CH$_4$/^{13}C	5.8 ± 0.9	5.0 ± 0.2
^{13}CH$_4$/C	7.6 ± 1.5	1.6 ± 0.1

[a] Natural abundance.

nitride clusterfullerene $Sc_3N@C_{80}$. Yet, absorption and fluorescence spectroscopy as well as electrochemical study show that the band-gap of $Sc_3CH@C_{80}$ is higher by 0.09 eV. Most importantly, a unique possibility to determine ^{13}C composition of the central atom in the cluster by ^{1}H NMR enables an analysis of the role of methane in the clusterfullerene formation. A series of ^{13}C enrichment with either [13]CH_4 or ^{13}C powder showed that the use of [13]CH_4 in the synthesis of $Sc_3CH@C_{80}$ allows selective enrichment of the central carbon atom with [13]C.

Notes and references

1 A. A. Popov, S. Yang and L. Dunsch, *Chem. Rev.*, 2013, **113**, 5989; X. Lu, L. Feng, T. Akasaka and S. Nagase, *Chem. Soc. Rev.*, 2012, **41**, 7723; A. Rodriguez-Fortea, A. L. Balch and J. M. Poblet, *Chem. Soc. Rev.*, 2011, **40**, 3551.

2 S. Stevenson, G. Rice, T. Glass, K. Harich, F. Cromer, M. R. Jordan, J. Craft, E. Hadju, R. Bible, M. M. Olmstead, K. Maitra, A. J. Fisher, A. L. Balch and H. C. Dorn, *Nature*, 1999, **401**, 55.

3 L. Dunsch, M. Krause, J. Noack and P. Georgi, *J. Phys. Chem. Solids*, 2004, **65**, 309; L. Dunsch, P. Georgi, M. Krause and C. R. Wang, *Synth. Met.*, 2003, **135**, 761.

4 N. Chen, M. N. Chaur, C. Moore, J. R. Pinzon, R. Valencia, A. Rodriguez-Fortea, J. M. Poblet and L. Echegoyen, *Chem. Commun.*, 2010, **46**, 4818; N. Chen, M. Mulet-Gas, Y.-Y. Li, R. E. Stene, C. W. Atherton, A. Rodriguez-Fortea, J. M. Poblet and L. Echegoyen, *Chem. Sci.*, 2013, **4**, 180; N. Chen, C. M. Beavers, M. Mulet-Gas, A. Rodriguez-Fortea, E. J. Munoz, Y.-Y. Li, M. M. Olmstead, A. L. Balch, J. M. Poblet and L. Echegoyen, *J. Am. Chem. Soc.*, 2012, **134**, 7851; F.-F. Li, N. Chen, M. Mulet-Gas, V. Triana, J. Murillo, A. Rodriguez-Fortea, J. M. Poblet and L. Echegoyen, *Chem. Sci.*, 2013, **4**, 3404.

5 T. Yang, Y. Hao, L. Abella, Q. Tang, X. Li, Y. Wan, A. Rodríguez-Fortea, J. M. Poblet, L. Feng and N. Chen, *Chem. – Eur. J.*, 2015, **21**, 11110; M. Zhang, Y. Hao, X. Li, L. Feng, T. Yang, Y. Wan, N. Chen, Z. Slanina, F. Uhlik and H. Cong, *J. Phys. Chem. C*, 2014, **118**, 28883; Q. Tang, L. Abella, Y. Hao, X. Li, Y. Wan, A. Rodríguez-Fortea, J. M. Poblet, L. Feng and N. Chen, *Inorg. Chem.*, 2015, **54**, 9845.

6 M. Krause, F. Ziegs, A. A. Popov and L. Dunsch, *ChemPhysChem*, 2007, **8**, 537.

7 A. L. Svitova, K. Ghiassi, C. Schlesier, K. Junghans, Y. Zhang, M. Olmstead, A. Balch, L. Dunsch and A. A. Popov, *Nat. Commun.*, 2014, **5**, 3568; Y. Feng, T. Wang, J. Wu, Z. Zhang, L. Jiang, H. Han and C. Wang, *Chem. Commun.*, 2014, **50**, 12166.

8 Q. Deng, K. Junghans and A. A. Popov, *Theor. Chem. Acc.*, 2015, **134**, 10.

9 K. Junghans, C. Schlesier, A. Kostanyan, N. A. Samoylova, Q. Deng, M. Rosenkranz, S. Schiemenz, R. Westerström, T. Greber, B. Büchner and A. A. Popov, *Angew. Chem., Int. Ed. Engl.*, 2015, **54**, 13411.

10 C. R. Wang, Z. Q. Shi, L. J. Wan, X. Lu, L. Dunsch, C. Y. Shu, Y. L. Tang and H. Shinohara, *J. Am. Chem. Soc.*, 2006, **128**, 6605.

11 Y.-Z. Tan, X. Han, X. Wu, Y.-Y. Meng, F. Zhu, Z.-Z. Qian, Z.-J. Liao, M.-H. Chen, X. Lu, S.-Y. Xie, R.-B. Huang and L.-S. Zheng, *J. Am. Chem. Soc.*, 2008, **130**, 15240; Y. Z. Tan, J. Li, F. Zhu, X. Han, W. S. Jiang, R. B. Huang, Z. P. Zheng, Z. Z. Qian, R. T. Chen, Z. J. Liao, S. Y. Xie, X. Lu and L. S. Zheng, *Nat. Chem.*, 2010, **2**, 269; S. Y. Xie, F. Gao, X. Lu, R. B. Huang, C. R. Wang, X. Zhang, M. L. Liu, S. L. Deng and L. S. Zheng, *Science*, 2004, **304**, 699; Y.-Z. Tan, R.-T. Chen, Z.-J. Liao, J. Li, F. Zhu, X. Lu, S.-Y. Xie, J. Li, R.-B. Huang and L.-S. Zheng, *Nat. Commun.*, 2011, **2**, 420; Y.-Z. Tan, S.-Y. Xie, R.-B. Huanh and I.-S. Zheng, *Nat. Chem.*, 2009, **1**, 450.

12 S. Yang, L. Zhang, W. Zhang and L. Dunsch, *Chem. – Eur. J.*, 2010, **16**, 12398; M. Jiao, W. Zhang, Y. Xu, T. Wei, C. Chen, F. Liu and S. Yang, *Chem. – Eur. J.*, 2012, **18**, 2666; F. Liu, J. Guan, T. Wei, S. Wang, M. Jiao and S. Yang, *Inorg. Chem.*, 2013, **52**, 3814.

13 X. Lu, T. Akasaka and S. Nagase, *Acc. Chem. Res.*, 2013, **46**, 1627; H. Kurihara, X. Lu, Y. Iiduka, N. Mizorogi, Z. Slanina, T. Tsuchiya, T. Akasaka and S. Nagase, *J. Am. Chem. Soc.*, 2011, **133**, 2382; J. Zhang, T. Fuhrer, W. Fu, J. Ge, D. W. Bearden, J. L. Dallas, J. C. Duchamp, K. L. Walker, H. Champion, H. F. Azurmendi, K. Harich and H. C. Dorn, *J. Am. Chem. Soc.*, 2012, **134**, 8487.

14 Y. Yamazaki, K. Nakajima, T. Wakahara, T. Tsuchiya, M. O. Ishitsuka, Y. Maeda, T. Akasaka, M. Waelchli, N. Mizorogi and H. Nagase, *Angew. Chem., Int. Ed. Engl.*, 2008, **47**, 7905.

15 J. Zhang, F. L. Bowles, D. W. Bearden, W. K. Ray, T. Fuhrer, Y. Ye, C. Dixon, K. Harich, R. F. Helm, M. M. Olmstead, A. L. Balch and H. C. Dorn, *Nat. Chem.*, 2013, **5**, 880.

16 T. Wang and C. Wang, *Acc. Chem. Res.*, 2014, **47**, 450.

17 T.-S. Wang, N. Chen, J.-F. Xiang, B. Li, J.-Y. Wu, W. Xu, L. Jiang, K. Tan, C.-Y. Shu, X. Lu and C.-R. Wang, *J. Am. Chem. Soc.*, 2009, **131**, 16646.

18 T.-S. Wang, L. Feng, J.-Y. Wu, W. Xu, J.-F. Xiang, K. Tan, Y.-H. Ma, J.-P. Zheng, L. Jiang, X. Lu, C.-Y. Shu and C.-R. Wang, *J. Am. Chem. Soc.*, 2010, **132**, 16362.

19 A. A. Popov, N. Chen, J. R. Pinzón, S. Stevenson, L. A. Echegoyen and L. Dunsch, *J. Am. Chem. Soc.*, 2012, **134**, 19607.

20 K. Kamieńska-Trela, in *Annu. Rep. NMR Spectrosc.*, ed. G. A. Webb, Academic Press, 1995, pp. 131.

21 K. Komatsu, M. Murata and Y. Murata, *Science*, 2005, **307**, 238.

22 K. Kurotobi and Y. Murata, *Science*, 2011, **333**, 613.

23 M. Murata, S. Maeda, Y. Morinaka, Y. Murata and K. Komatsu, *J. Am. Chem. Soc.*, 2008, **130**, 15800.

24 A. Krachmalnicoff, R. Bounds, S. Mamone, M. H. Levitt, M. Carravetta and R. J. Whitby, *Chem. Commun.*, 2015, **51**, 4993; E. E. Maroto, J. Mateos, M. Garcia-Borràs, S. Osuna, S. Filippone, M. Á. Herranz, Y. Murata, M. Solà and N. Martín, *J. Am. Chem. Soc.*, 2015, **137**, 1190.

25 X. Lu, K. Nakajima, Y. Iiduka, H. Nikawa, N. Mizorogi, Z. Slanina, T. Tsuchiya, S. Nagase and T. Akasaka, *J. Am. Chem. Soc.*, 2011, **133**, 19553.

26 S. Yang, C. Chen, F. Liu, Y. Xie, F. Li, M. Jiao, M. Suzuki, T. Wei, S. Wang, Z. Chen, X. Lu and T. Akasaka, *Sci. Rep.*, 2013, **3**, 1487.

27 A. A. Popov and L. Dunsch, *Chem. – Eur. J.*, 2009, **15**, 9707.

28 J. P. Perdew, K. Burke and M. Ernzerhof, *Phys. Rev. Lett.*, 1996, **77**, 3865; F. Neese, *WIREs Comput. Mol. Sci.*, 2012, **2**, 73; W. Humphrey, A. Dalke and K. Schulten, *J. Mol. Graphics*, 1996, **14**, 33.

29 H. Lange, K. Saidane, M. Razafinimanana and A. Gleizes, *J. Phys. D: Appl. Phys.*, 1999, **32**, 1024.